

Accumulation of 8-oxodG within the human mitochondrial genome positively associates with transcription

Giovanni Scala^{1,†}, Susanna Ambrosio^{1,†}, Margherita Menna¹, Francesca Gorini², Carmen Caiazza¹, Marcus S. Cooke³, Barbara Majello¹ and Stefano Amente^{2,*}

¹Department of Biology, University of Naples Federico II, 80138 Naples, Italy

²Department of Molecular Medicine and Medical Biotechnologies, University of Naples Federico II, 80131 Naples, Italy

³Oxidative Stress Group, Department of Molecular Biosciences, University of South Florida, Tampa, FL 33620, USA

*To whom correspondence should be addressed. Tel: +39 081 7463044; Email: stamente@unina.it

†The authors wish it to be known that, in their opinion, the first two authors should be regarded as Joint First Authors.

Abstract

Mitochondrial DNA (mtDNA) can be subject to internal and environmental stressors that lead to oxidatively generated damage and the formation of 8-oxo-7,8-dihydro-2'-deoxyguanine (8-oxodG). The accumulation of 8-oxodG has been linked to degenerative diseases and aging, as well as cancer. Despite the well-described implications of 8-oxodG in mtDNA for mitochondrial function, there have been no reports of mapping of 8-oxodG across the mitochondrial genome. To address this, we used OxiDIP-Seq and mapped 8-oxodG levels in the mitochondrial genome of human MCF10A cells. Our findings indicated that, under steady-state conditions, 8-oxodG is non-uniformly distributed along the mitochondrial genome, and that the longer non-coding region appeared to be more protected from 8-oxodG accumulation compared with the coding region. However, when the cells have been exposed to oxidative stress, 8-oxodG preferentially accumulated in the coding region which is highly transcribed as H1 transcript. Our data suggest that 8-oxodG accumulation in the mitochondrial genome is positively associated with mitochondrial transcription.

Introduction

Mitochondrial DNA (mtDNA) is a circular genome consisting of multiple copies and encoding 13 crucial subunits of the mitochondrial respiratory chain, along with two rRNAs (12S and 16S) and 22 tRNAs (Figure 1A) (1–4).

mtDNA plays a crucial role in cellular energy production and is highly susceptible to damage caused by reactive oxygen species (ROS) (5), which can lead to the formation of 8-oxo-7,8-dihydro-2'-deoxyguanine (8-oxodG) (6). 8-oxodG in mtDNA, as well as in nuclear DNA (nDNA), is primarily repaired by the base excision repair (BER) pathway (7), but incomplete repair can lead to mutagenesis and genome instability (6). OGG1, the enzyme responsible for catalyzing the removal of the 8-oxodG, is encoded within the nuclear genome. Intriguingly, both mitochondrial and nuclear transcript isoforms originate from the same gene (8). Consequently, the regulation of OGG1 expression in both the mitochondria and nucleus exhibits overlapping characteristics. The presence of 8-oxodG in mtDNA has been linked to the development of degenerative diseases (9), cardiovascular disease (9), aging (10–12) and cancer (13).

Interestingly, recent studies have reported that 8-oxodG accumulation in the nuclear genome plays a role in the epigenetic regulation of gene expression (14). However, the impact of 8-oxodG in the context of mitochondrial transcription remains largely unexplored. Mitochondrial transcription is a pivotal process orchestrated by a dedicated transcription machinery. The proteins comprising this transcriptional machinery differ from those forming the machinery involved in nuclear tran-

scription, even though all of them are encoded within the nucleus (15,16). Unlike nuclear genes which often possess multiple specialized promoters, mitochondrial transcription initiates within one regulatory region, namely the non-coding region (NCR), and results in the generation of three polycistronic transcripts originating from the heavy-strand promoter 1 (HSP1), HSP2 and light-strand promoter (LSP) regions within the mitochondrial genome (Figure 1B) (17–19).

Despite the established potential for 8-oxodG in DNA to affect cell function (6,20,21), the full extent of the impact of 8-oxodG on mitochondrial function remains incompletely understood. Thus, exploring the distribution of 8-oxodG within the mitochondrial genome could greatly enhance our understanding of how 8-oxodG impacts mitochondrial homeostasis.

Here, we present a study which utilizes OxiDIP-Seq (22–25) to perform a high-resolution mapping of 8-oxodG across the mitochondrial genome of human MCF10A cells. This study is the first to map 8-oxodG across the human mitochondrial genome. We have uncovered novel insights into the patterns of 8-oxodG distribution and accumulation within the mitochondrial genome under steady-state conditions, in untreated cells and following oxidative stress.

Our findings reveal a potential association between 8-oxodG accumulation and transcription-related processes in mitochondria. Understanding the mechanisms underlying 8-oxodG accumulation/repair in mtDNA, and its role in mitochondrial transcription, may pave the way for the development of targeted therapeutic strategies aimed at mitigating the

Received: July 21, 2023. Revised: October 3, 2023. Editorial Decision: October 23, 2023. Accepted: October 25, 2023

© The Author(s) 2023. Published by Oxford University Press on behalf of NAR Genomics and Bioinformatics.

This is an Open Access article distributed under the terms of the Creative Commons Attribution-NonCommercial License

(<http://creativecommons.org/licenses/by-nc/4.0/>), which permits non-commercial re-use, distribution, and reproduction in any medium, provided the original work is properly cited. For commercial re-use, please contact journals.permissions@oup.com

effects of oxidative stress, by preserving mitochondrial function, and hence mitigating the risk of several diseases.

Materials and methods

Cell culture and treatments

MCF10A cells were cultured in a 1:1 mixture of Dulbecco's modified Eagle's medium (DMEM)-F12 supplemented with 5% horse serum, 10 µg/ml insulin, 0.5 µg/ml hydrocortisone, 20 ng/ml epidermal growth factor and 100 ng/ml cholera enterotoxin, and incubated at 37°C in a humidified atmosphere with 5% CO₂ (22). To perform the UV radiation (UVR) treatment, MCF10A cells in exponential growth phase were subjected to UV light (254 nm) for a total dose of 40 J/m² (22). Following irradiation, the medium was replaced, and the cells were incubated at 37°C for 30 min for recovery. Subsequently, the cells were rinsed twice with ice-cold phosphate-buffered saline (PBS) and harvested. For *N*-acetyl cysteine (NAC) treatment, the medium was supplemented with 1 mM NAC (Sigma) and incubated for 1 h at 37°C (22).

4-Thiouridine incorporation assay

For RNA labeling, 4-thiouridine (Sigma) was added directly to the growth medium at a final concentration of 400 µM and incubated for 30 min. Total RNA was isolated using Tri-Fast II reagent (Euroclone). DNase I treatment (New England Biolabs) was performed according to the manufacturer's instructions, followed by phenol/chloroform extraction; an aliquot of total RNA was saved for Input samples. RNA was quantified using a Qubit 4 (Invitrogen) and fragmented using the Bioruptor Pico (Diagenode) sonication device, with the following settings: one cycle, 30 s ON/30 s OFF. An 80 µg aliquot of fragmented RNA in 250 µl of RNase-free water was used for the biotinylation reaction. Biotinylation of 4sU-labeled RNA was performed by addition to RNA samples of the following reagents: 100 µl of EZ-LinkBiotin-HPDP (Pierce) dissolved in dimethylformamide at a final concentration of 1 mg/ml; 50 µl of 10× biotinylation buffer (100 mM Tris pH 7.5, 10 mM EDTA); and 100 µl of dimethylformamide (DMF). Biotinylation was carried out at 24°C for 2 h. Unbound biotin-HPDP was removed by chloroform extraction. A 1/10 volume of 5 M NaCl and an equal volume of isopropanol were then added, and RNA was precipitated at 16 000 g for 5 min at 4°C. The pellet was washed with an equal volume of 75% ethanol and precipitated again at 4°C for 15 min, and then resuspended in 100 µl of RNase-free water. RNA samples were denatured by heating at 65°C for 10 min, rapidly cooled on ice for 5 min and incubated with 50 µl of M280 streptavidin Dynabeads (Invitrogen) with rotation for 15 min at 4°C. The Dynabeads were then washed three times with 1 ml of 65°C wash buffer (100 mM Tris-HCl pH 7.5, 10 mM EDTA pH 8.0, 1 M NaCl, 0.1% Tween-20), followed by three washes with room temperature wash buffer. Labeled RNA was eluted by the addition of 100 µl of freshly prepared 100 mM dithiothreitol. RNA was recovered from the wash fractions and purified using the RNA Clean and Purification Kit (Zymo Research). Unlabeled RNA sample was added to parallel reactions as negative control.

Quantitative polymerase chain reaction (qPCR)

cDNA from total RNA (Input) was synthesized using LunaScript (New England Biolabs) according to the manu-

facturer's instructions. For labeled RNA samples, cDNA was synthesized using the Ultra II directional RNA Libraryprep Kit for Illumina (New England Biolabs). The level of nuclear glyceraldehyde phosphate dehydrogenase (GAPDH) mRNA in total RNA samples was used as an internal control. qPCR was performed using a AriaMax (Agilent) detection system with SYBR green (Brilliant III Ultra-Fast SYBR Green Agilent) incorporation with the following primers: GAPDH_Fw, CCA-CATCGCTCAGACACCAT; GAPDH_Rev, CCAGGCGC-CCAATACG; MT-RNR2_Fw, CATAAGCCTGCGTCAGATCA; MT-RNR2_Rev, CCTGTGTTGGGTTGACAGTG; MT-ND5_Fw, AGTTACAATCGGCATCAACCAA; MT-ND5_Rev, CCCGGAGCACATAAATAGTATGG.

Bioinformatics and statistical analyses

8-oxodG levels in untreated MCF10A cells were obtained previously (22) and the raw data can be downloaded from the Sequence Read Archive (SRA; PRJNA391133). 8-oxodG levels in UVR-treated MCF10A cells were obtained previously (24) and the raw data can be downloaded from the SRA (PRJNA798917). 8-oxodG levels for NAC-treated MCF10A cells were obtained previously (24) and the raw data can be downloaded from the SRA (PRJNA798917). 8-oxodG levels in mtDNA were obtained for each of the above conditions and corresponding input by first pre-processing all fastq files as in (24), then using *bwa aln* with default parameters to align reads against the hg18 reference genome including mtDNA, and then removing duplicates using *picard MarkDuplicates*. We extracted from each of the .bam files all the reads mapping to mtDNA using *samtools view* and normalized the signal passing *OxiDIP-Seq chrM bam* files along with the corresponding input bam file to *deepTools bamCompare* using *-exactScaling -p max* options and converted them to bigwig format using the *bigWigToBedGraph* command. GC content was obtained by downloading the *gc5Base* track from the UCSC genome browser in bed format and converting it into bigwig format using *bedGraphToBigWig*. mtDNA G4-rich region coordinates in HEK293 cells were extracted from (26), compiled as a bed file and converted to bigwig format using *bigWigToBedGraph*.

To measure and compare average 8-oxodG levels between mtDNA and nDNA in each of the experimental conditions (untreated, UV and NAC treated), we used *wiggletools* to perform the following chain of operation starting from the bigwig files containing normalized 8-oxodG signal (chrM or nDNA): (i) binning of the signal using 50 bp windows size; (ii) computation of the average 8-oxodG value for each bin; and (iii) computation of total mean, standard deviation and number of bins. For each condition, we used these statistics computed over chrM and nDNA to perform a Welch *t*-test in R.

The relationship between the GC content and 8-oxodG levels in each condition was investigated by first binning the two signals over the same genomic coordinates using a fixed window approach with *deepTools multiBigwigSummary* over the two bigwig files with *-outRawCounts* option and finally importing the two output tables into R to compute Pearson's correlations. The relationship between G4-rich regions and 8-oxodG levels has been investigated for each tested condition by extrapolating (i) the normalized chrM 8-oxodG levels in G4-enriched regions and (ii) the normalized chrM 8-oxodG levels in the complement of mtDNA regions to G4 regions using *bedtools intersect* and *bedtools diff* commands,

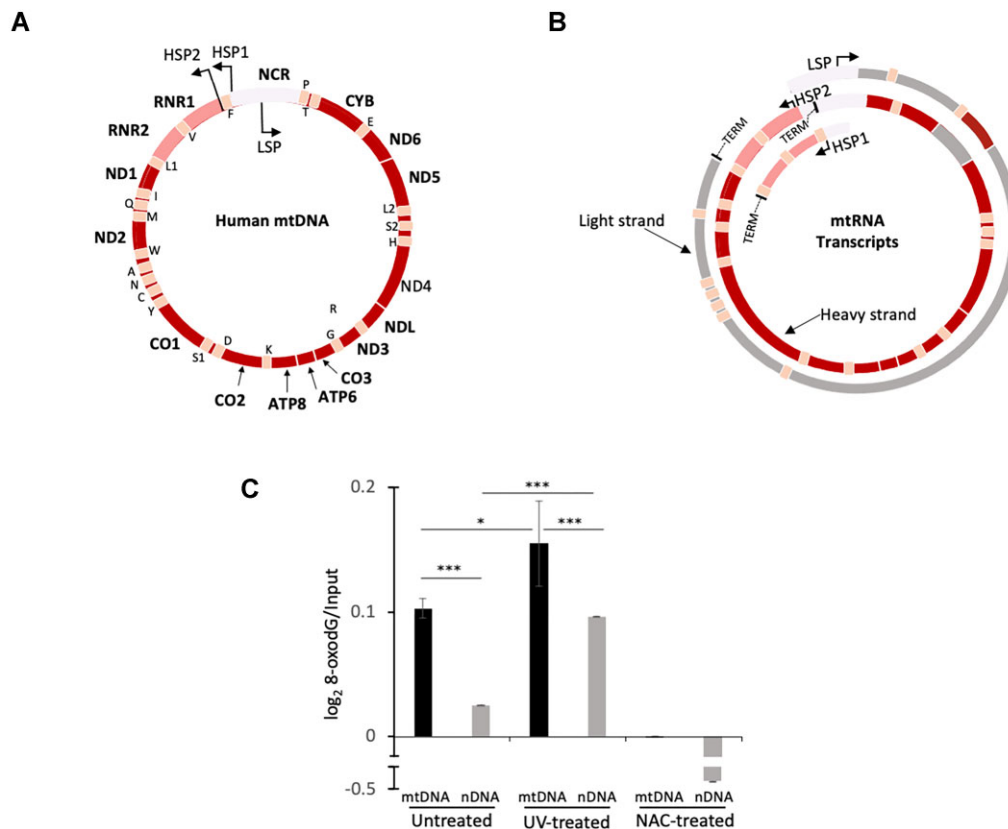


Figure 1. (A) Schematic representation of the human mitochondrial genome. The genetic information within mtDNA is densely packed and actively transcribed. The mtDNA regulatory region is the only substantial non-coding region (NCR). Arrows indicate promoters: LSP, light-strand promoter; HSP, heavy-strand promoter. Uppercase letters indicate tRNAs; and RNR1 and RNR2 indicate rRNAs 12S and 16S respectively; CO1, cytochrome *c* oxidase subunit I; CO2, cytochrome *c* oxidase subunit II; CO3, cytochrome *c* oxidase subunit III; CYB, cytochrome *b*; ND1–6, NADH dehydrogenase subunits 1–6. (B) Schematic representation of the mitochondrial polycistronic transcripts. Mitochondrial transcription initiation occurs in the NCR, which contains two promoters located on the heavy (HSP1 and HSP2) and one promoter on the light strand (LSP) for mtDNA transcription, and various conserved sequences responsible for regulatory functions. Three different polycistronic transcripts, H1, H2 and L, generated through transcription from the HSP1, HSP2 and LSP promoters, respectively, are indicated. The LSP is responsible for transcribing eight tRNAs and the MT-ND6 gene. The heavy strand utilizes HSP1 and HSP2, and transcription from HSP1 results in a transcript encompassing tRNA^{Phe}, tRNA^{Val} and the two rRNAs (12S and 16S). In contrast, transcription originating from HSP2 produces a transcript coding the two rRNAs, 12 proteins and 14 tRNAs. TERM indicates putative termination sites for H1, H2 and L transcription. (C) Average signal of normalized 8-oxodG in mitochondrial and nuclear DNA in untreated and UVR-, and NAC-treated MCF10A cells. Data are presented as mean values \pm 2 SEM, ** $P = 3.1 \times 10^{-3}$, *** $P < 2.2 \times 10^{-22}$.

respectively, and then testing the difference between average 8-oxodG levels in these two groups using Welch *t*-test in R.

The difference in average 8-oxodG levels between the NCR and coding region has been investigated for each tested condition by first subsetting (i) the normalized chrM 8-oxodG levels in NCR and (ii) the normalized chrM 8-oxodG levels in the complementary coding region of mtDNA regions, and then testing the difference between average 8-oxodG levels in these two groups using Welch *t*-test in R.

This study used 0.05 as the significance threshold; all statistical analyses have been performed with R (<https://www.R-project.org/>).

Results

Comparison of the 8-oxodG levels in mitochondrial and nuclear DNA determined by OxiDIP-seq

We have recently developed and applied the OxiDIP-Seq method to describe the 8-oxodG distribution across the human nuclear genome (22–25). Our initial focus was on the nuclear genome, like much of the literature [except for Wau-

chope *et al.* (27) and a later report from ourselves (28) both of which also considered the mitochondrial genome]. However, in our previous experiments, OxiDIP-Seq data were generated from the entire genome (both nDNA and mtDNA molecules) of human MCF10A cells, giving us the opportunity to retrospectively examine the distribution of 8-oxodG across the mitochondrial genome.

Firstly, we measured the average signal of normalized 8-oxodG levels in mtDNA and compared this with nDNA in untreated and in UVR- or NAC-treated MCF10A cells. UV- and NAC-based treatments have been used previously to modulate the genomic levels of 8-oxodG, which increase as a result of oxidative stress induced by UVR exposure (22) and decrease due to the ROS-scavenging capability of NAC (22,24). In the untreated cells, i.e. cells in redox steady state, we observed that mtDNA had a higher (~4-fold) average oxidation level compared with nDNA (Figure 1C). These data are consistent with previously reported findings that indicate a higher susceptibility of mtDNA to oxidatively generated DNA damage compared with nDNA (5,29). However, when the cells were exposed to UVR-induced oxidative stress, we observed a significant increase in 8-oxodG levels in both mtDNA and, as

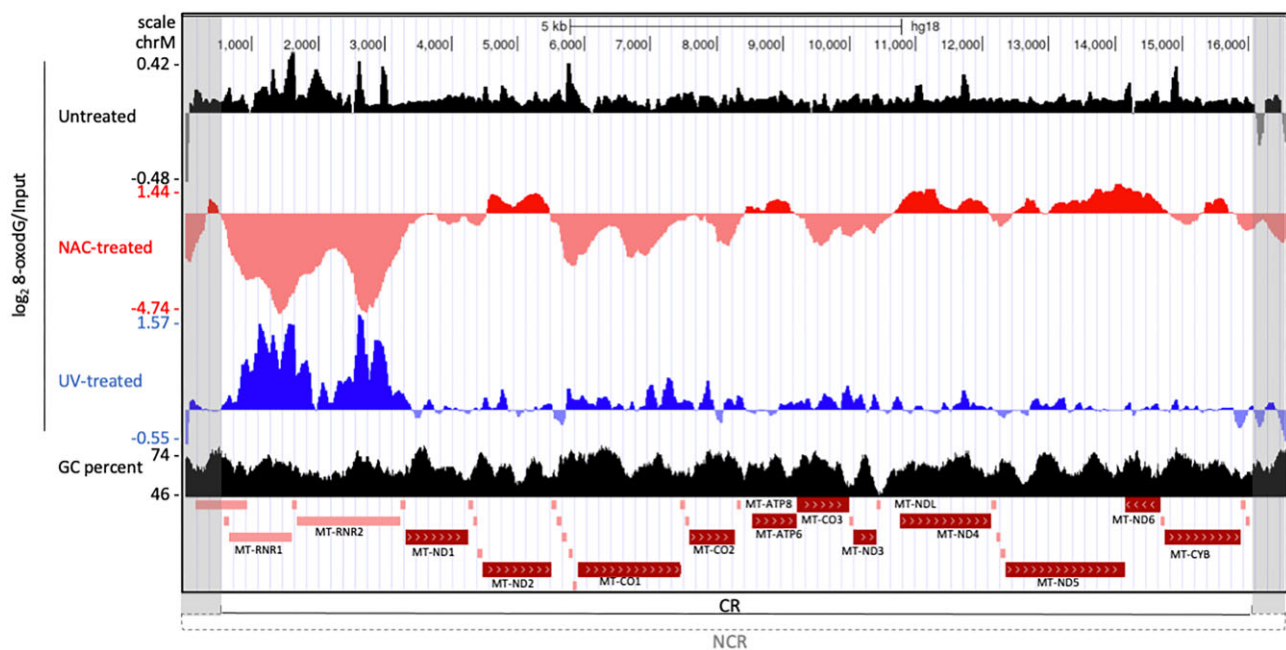


Figure 2. UCSC visualization of 8-oxodG mapping in the mtDNA in untreated (black, top), NAC-treated (red) and UVR-treated (blue) MCF10A cells; the panel also includes the GC percent (black, bottom) and annotated the NCR (gray shaded area) and the coding region (CR). The CR contains rRNAs and tRNAs (light red) and coding proteins (dark red) genes.

previously demonstrated (22), nDNA. Notably, the increase in 8-oxodG following UVR treatment was higher in nDNA compared with mtDNA (Figure 1C). Finally, the treatment with the antioxidant NAC decreased the endogenous levels of 8-oxodG in both mtDNA and nDNA (Figure 1C), in agreement with previous findings reported for the nuclear genome (22–24).

Overall, these data demonstrate that the average 8-oxodG level is higher in mtDNA compared with nDNA, both under steady-state redox conditions and during UVR-induced oxidative stress.

Distribution of 8-oxodG in mitochondrial DNA

To examine the 8-oxodG distribution in mtDNA, we used the UCSC genome browser and visualized the 8-oxodG mitochondrial signal from untreated MCF10A cells (Figure 2). We observed a non-uniform distribution of the 8-oxodG signal along the entire mtDNA genome, with multiple 8-oxodG peaks within the region containing *RNR1* and *RNR2* genes (encoding the 12S and 16S rRNAs, respectively, Figure 2, upper, black-colored track). Next, as 8-oxodG accumulation has been reported to occur at gene regulatory regions in the nuclear genome (22,23), we considered whether this might also occur in the mitochondria NCR (Figure 2, gray shaded area) as this region hosts the *O_H* and *HSP1*, *HSP2* and *LSP*. We therefore re-plotted the 8-oxodG mitochondrial signal using the R platform (Supplementary Figure S1A) and, by visual inspection, we observed a lower level of the normalized 8-oxodG signal at the NCR compared with the coding region. To confirm this, we measured the average 8-oxodG values in the NCR versus the entire coding region of the mtDNA and found lower 8-oxodG levels in the NCR (mean = 0.02 and 0.11, NCR and coding region, respectively, $P = 0.01$ Welch t -test; Supplementary Figure S1B).

Subsequently, we also visualized the 8-oxodG signal derived from the NAC- and UVR-treated cells (Figure 2). As expected, and in agreement with the data in Figure 1C, we observed a broad and highly evident decrease in 8-oxodG signal across the entire mitochondrial genome in NAC-treated cells (Figure 2, red-colored track). Similarly, we observed an increase in the 8-oxodG levels following the induction of oxidative stress by UVR (Figure 2, blue-colored track). However, the resulting increase in 8-oxodG levels was exclusively restricted to the coding sequences encompassing *RNR1* and *RNR2* genes (Figure 2, blue-colored track). Furthermore, the NCR again showed a lower 8-oxodG signal compared with the region encompassing *RNR1* and *RNR2* genes (mean = -0.05 and 0.6 , NCR and coding region, respectively, $P = 4.8e-16$ Welch t -test; Supplementary Figure S2A, B).

Since previous studies have indicated a relationship between the accumulation of 8-oxodG in the nuclear genome and genomic features such as GC content and G4 structures (23), we compared the mitochondrial 8-oxodG signal from untreated MCF10A cells with the GC percent and G4-enriched regions previously identified in mitochondria (26). First, we performed a Pearson's correlation analysis that revealed no significant correlation between the 8-oxodG signal and GC content ($r = -0.04$). Then, we measured the average 8-oxodG levels in G4-enriched regions and the complementary G4-poor regions and found only a slight difference (median = 0.09 and 0.1, G4-enriched and G4-poor regions, respectively, $P = 0.008$ Welch t -test; Supplementary Figure S3). Hence, these findings suggest that the accumulation of 8-oxodG is not associated with the GC content or G4 structures in mitochondria.

Overall, these data showed a non-uniform distribution of high 8-oxodG levels at the coding region and lower 8-oxodG levels at the regulatory regions under steady-state conditions. However, following oxidative stress, high 8-oxodG levels

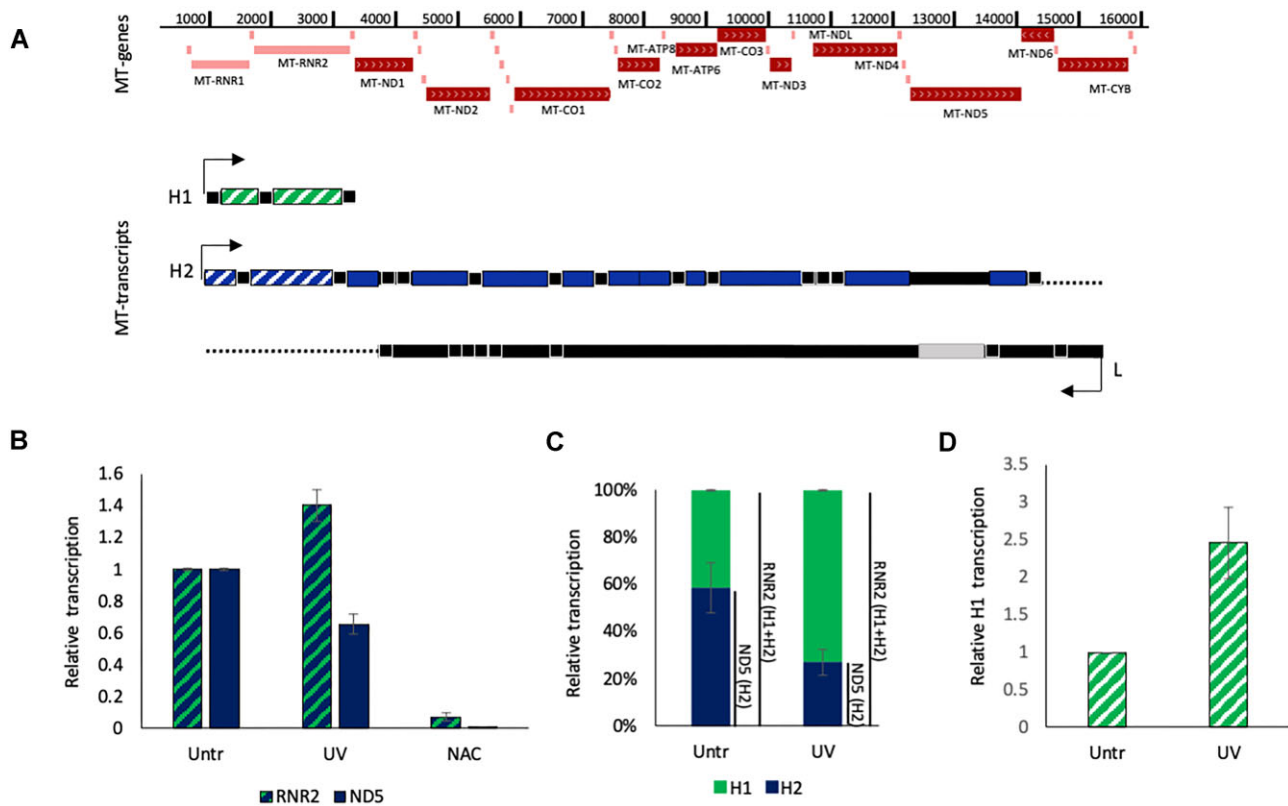


Figure 3. (A) Schematic representation of the mitochondrial polycistronic transcripts H1, H2 and L. For (B–D) we used thiol-specific biotinylation of 4sU-labeled RNA, followed by streptavidin-based enrichment, to isolate newly synthesized transcripts. (B) RT-qPCR analyses show relative transcription of the RNR2 and ND5 RNAs in biotinylated samples treated with UVR (UV) or NAC, or left untreated (Untr). (C) Relative transcription levels of the H1 and H2 transcripts in untreated and UVR-treated cells (D) Relative H1 transcript level in untreated and UVR-treated cells. Data are normalized to the nuclear GAPDH mRNA in total RNA inputs. The analyses were conducted twice and are presented as the mean \pm SD.

preferentially accumulated at the region encompassing the *RNR1* and *RNR2* genes. Moreover, GC content and G4 structures were not associated with the accumulation of high 8-oxodG levels.

8-oxodG levels positively associate with the transcription of mitochondrial DNA

We found that the main genome structural features such as GC content and G4 structures, which have been linked previously to 8-oxodG levels in the nuclear genome (23), did not appear to play a significant role in determining the sites of 8-oxodG accumulation in the mitochondrial genome. However, we observed that 8-oxodG accumulation occurs preferentially in the *RNR1* and *RNR2* genes and overlaps with a region that is transcribed even in the shorter polycistronic transcript H1 (17–19) (Figure 3A). This led us to hypothesize that transcription of the H1 transcript might contribute to the distribution of mitochondrial 8-oxodG accumulation. To investigate this hypothesis, we performed a 4sU incorporation experiment in untreated and UVR- or NAC-treated MCF10A cells and measured the transcription level of the two mitochondrial polycistronic transcripts H1 and H2 (Figure 3A).

First, we assessed the transcription level of the *RNR2* gene, which can be transcribed from both H1 and H2 transcripts, as well as of the *ND5* gene which is exclusively transcribed from the H2 transcript (Figure 3A). Comparing UVR-treated with untreated cells, we found that the *RNR2* gene showed an increase in the level of transcription, while the *ND5* gene dis-

played a decrease in transcription (Figure 3B). This suggests that the H1 transcript is more actively transcribed in UVR-treated cells compared with untreated cells, while the H2 transcript is less transcribed under these conditions.

To confirm this, we aimed to quantify the relative transcription levels of the H1 and H2 transcripts by subtracting the transcription level of *ND5* (H2) from that of *RNR2* (H1 + H2). In untreated cells, we discovered that ~60% (Figure 3C, Untr, blue bar) of the RNAs transcribed for the *RNR2* gene originated from the H2 transcripts, while ~40% (Figure 3C, Untr, green bar) of the *RNR2* transcript is derived from the H1 transcript. However, in UVR-treated cells, the *RNR2* gene was transcribed 27% (Figure 3C, UV, blue bar) from the H2 transcript and the remaining 73% (Figure 3C, UV, green bar) from the H1 transcript. Consequently, comparing UVR-treated with untreated cells, the levels of the H2 transcript decreased by a factor of 2.2 (60/27) (blue bars in Figure 3C), and the levels of the H1 transcript increased by a factor of 2.5 (Figure 3D). Overall, this analysis suggests that the increased levels of 8-oxodG observed in the region containing the *RNR1* and *RNR2* genes are associated with higher transcription levels of the mitochondrial H1 transcript in UV-treated cells.

Finally, we observed a significant decrease in the transcription levels of both *RNR2* and *ND5* genes in NAC-treated cells compared with untreated cells (Figure 3B). This finding further confirms the connection between the substantial reduction in 8-oxodG levels and decreased transcription levels in the mitochondria. Taken together, these data suggest that the

accumulation of 8-oxodG is positively associated with transcription in mitochondria.

Discussion

mtDNA is essential for cellular energy production but is susceptible to oxidatively generated damage which can result in lesions such as 8-oxodG (5,6). The presence of 8-oxodG in mtDNA has been associated with various diseases (9–13). However, there is still limited understanding regarding how and where the localization of 8-oxodG in the mitochondrial genome impacts mitochondrial function. To address this gap in the literature, we conducted the present study using a previously unexplored subset of mitochondrial-associated data from the publicly available OxiDIP-Seq dataset (22–25), focusing on 8-oxodG in the mitochondrial genome.

Our findings revealed, for the first time, intriguing patterns of 8-oxodG distribution in the mitochondrial genome of human MCF10A cells under normal physiological (redox steady state), oxidative stress and antioxidant conditions. Under redox steady state, we observed a non-uniform distribution of 8-oxodG levels across the mitochondrial genome, as has been noted for cyclobutane pyrimidine dimers (CPDs) (28), although not for the malondialdehyde-dG adducts (M1dG) (27). In general, two dynamic processes contribute to the genome distribution of the DNA damage: (i) factors influencing where and how the damage forms and (ii) factors influencing local DNA repair machinery recruitment. These two processes may play distinct roles in managing non-bulky damage, like 8-oxodG which does not inherently cause transcription blockage (30), and bulky damage, as is the case for CPDs and M1dG which lead to RNA polymerase II stalling (31,32). This distinction could potentially account for the similarities or differences observed in the mitochondrial distribution patterns of 8-oxodG compared with CPDs or M1dG, respectively. Interestingly, the accumulation of 8-oxodG levels in mtDNA did not appear to be associated with sequence-linked features such as GC content and G4 structures, unlike nDNA (23). This observation provides additional evidence for the notion that biological processes involving DNA as substrate may have a role in mtDNA 8-oxodG accumulation.

We also analyzed OxiDIP-Seq data from cells exposed to oxidative stress induced by UV irradiation, as a biologically relevant source of increased ROS. Remarkably, we found that oxidative stress resulted in increased levels of 8-oxodG preferentially localized to a short region of the mtDNA, encompassing the *RNR1* and 2 genes and transcribed as the polycistronic transcript H1. Furthermore, following oxidative stress, we observed an increased rate of transcription of the H1 transcript. Conversely, decreasing mtDNA DNA 8-oxodG levels, through treatment with the antioxidant NAC, led to a decrease in mitochondrial transcription. These observations suggest a positive relationship between 8-oxodG levels and mitochondrial transcription, highlighting the necessity for conducting additional research to gain a deeper understanding of this association.

Surprisingly, in contrast to nuclear DNA (22,23), the promoters and replication origin located in the NCR exhibited significantly lower levels of 8-oxodG accumulation compared with the coding region, both under steady-state conditions and following oxidative stress. This indicates that these regulatory regions may be better protected against oxidatively generated damage by some form of safeguarding mechanisms (e.g. some form of physical protection against ROS formation

of 8-oxodG, and/or preferential DNA repair at these regions) or that the mechanisms involved in the production of 8-oxodG residues occur more easily in the coding region.

Our study provides evidence for a functional positive link between 8-oxodG accumulation and mitochondrial transcription, and opens up new avenues for exploring the cause-and-effect relationship between 8-oxodG and transcription in the mitochondrial genome. Additionally, it highlights the need for further investigation into the mechanisms underlying the accumulation and repair of 8-oxodG in mtDNA. This knowledge could potentially advance the development of therapeutic approaches aimed at mitigating the detrimental impacts of oxidative stress and preserving mitochondrial function.

Data availability

The datasets analyzed in this study are publicly available in the Gene Expression Omnibus (<https://www.ncbi.nlm.nih.gov/geo/>) with accessions GSE100234 and GSE194053

Supplementary data

Supplementary Data are available at NARGAB Online.

Acknowledgements

Author contributions: G.S. and M.M. performed bioinformatics analysis and statistical analyses; S.A., F.G. and C.C. carried out experiments; M.S.C. and B.M. contributed to data interpretation. S.A. (Stefano Amente) conceived the study and wrote the manuscript. All the authors contributed to the review, editing and revision of the final version of the manuscript. All authors have read and agreed to the published version of the manuscript.

Funding

The ‘Programma per il Finanziamento della Ricerca di Ateneo Linea A’ (FRA) 2022 (University of Naples Federico II) to Stefano Amente and GS; National Center for Gene Therapy and Drugs based on RNA Technology [CN00000041 PNR, MUR, Italy to Stefano Amente and BM]; AIRC [IG 23066 to B.M]; the National Institute of Environmental Health Sciences of the National Institutes of Health [R01ES030557 to M.S.C.]. The content is solely the responsibility of the author(s) and does not necessarily represent the official views of the National Institutes of Health.

Conflict of interest statement

None declared.

References

- Anderson, S., Bankier, A.T., Barrell, B.G., de Bruijn, M.H.L., Coulson, A.R., Drouin, J., Eperon, I.C., Nierlich, D.P., Roe, B.A., Sanger, F., *et al.* (1981) Sequence and organization of the human mitochondrial genome. *Nature*, 290, 457–465.
- Bonawitz, N.D., Clayton, D.A. and Shadel, G.S. (2006) Initiation and beyond: multiple functions of the human mitochondrial transcription machinery. *Mol. Cell*, 24, 813–825.
- Falkenberg, M., Larsson, N.-G. and Gustafsson, C.M. (2007) DNA replication and transcription in mammalian mitochondria. *Annu. Rev. Biochem.*, 76, 679–699.

4. Kasiviswanathan,R., Collins,T.R.L. and Copeland,W.C. (2012) The interface of transcription and DNA replication in the mitochondria. *Biochim. Biophys. Acta*, **1819**, 970–978.
5. Yakes,F.M. and Van Houten,B. (1997) Mitochondrial DNA damage is more extensive and persists longer than nuclear DNA damage in human cells following oxidative stress. *Proc. Natl Acad. Sci. USA*, **94**, 514–519.
6. Gorini,F., Scala,G., Cooke,M.S., Majello,B. and Amente,S. (2021) Towards a comprehensive view of 8-oxo-7,8-dihydro-2'-deoxyguanosine: highlighting the intertwined roles of DNA damage and epigenetics in genomic instability. *DNA Repair (Amst.)*, **97**, 103027.
7. Cooke,M.S., Olinski,R. and Loft,S. (2008) Measurement and meaning of oxidatively modified DNA lesions in urine. *Cancer Epidemiol. Biomarkers Prev.*, **17**, 3–14.
8. Nishioka,K., Ohtsubo,T., Oda,H., Fujiwara,T., Kang,D., Sugimachi,K. and Nakabeppu,Y. (1999) Expression and differential intracellular localization of two major forms of human 8-oxoguanine DNA glycosylase encoded by alternatively spliced OGG1 mRNAs. *Mol. Biol. Cell*, **10**, 1637–1652.
9. Tritschler,H.-J. and Medori,R. (1993) Mitochondrial DNA alterations as a source of human disorders. *Neurology*, **43**, 280–280.
10. Ames,B.N., Shigenaga,M.K. and Hagen,T.M. (1993) Oxidants, antioxidants, and the degenerative diseases of aging. *Proc. Natl Acad. Sci. USA*, **90**, 7915–7922.
11. Shigenaga,M.K., Hagen,T.M. and Ames,B.N. (1994) Oxidative damage and mitochondrial decay in aging. *Proc. Natl Acad. Sci. USA*, **91**, 10771–10778.
12. Wallace,D.C., Shoffner,J.M., Trounce,I., Brown,M.D., Ballinger,S.W., Corral-Debrinski,M., Horton,T., Jun,A.S. and Lott,M.T. (1995) Mitochondrial DNA mutations in human degenerative diseases and aging. *Biochim. Biophys. Acta*, **1271**, 141–151.
13. Li,C., Xue,Y., Ba,X. and Wang,R. (2022) The role of 8-oxoG repair systems in tumorigenesis and cancer therapy. *Cells*, **11**, 3798.
14. Gorini,F., Ambrosio,S., Lania,L., Majello,B. and Amente,S. (2023) The intertwined role of 8-oxodG and G4 in transcription regulation. *Int. J. Mol. Sci.*, **24**, 2031.
15. Basu,U., Bostwick,A.M., Das,K., Dittenhafer-Reed,K.E. and Patel,S.S. (2020) Structure, mechanism, and regulation of mitochondrial DNA transcription initiation. *J. Biol. Chem.*, **295**, 18406–18425.
16. Mercer,T.R., Neph,S., Dinger,M.E., Crawford,J., Smith,M.A., Shearwood,A.-M.J., Haugen,E., Bracken,C.P., Rackham,O., Stamatoyannopoulos,J.A., *et al.* (2011) The human mitochondrial transcriptome. *Cell*, **146**, 645–658.
17. Chang,D.D. and Clayton,D.A. (1984) Precise identification of individual promoters for transcription of each strand of human mitochondrial DNA. *Cell*, **36**, 635–643.
18. Montoya,J., Christianson,T., Levens,D., Rabinowitz,M. and Attardi,G. (1982) Identification of initiation sites for heavy-strand and light-strand transcription in human mitochondrial DNA. *Proc. Natl Acad. Sci. USA*, **79**, 7195–7199.
19. Montoya,J., Gaines,G.L. and Attardi,G. (1983) The pattern of transcription of the human mitochondrial rRNA genes reveals two overlapping transcription units. *Cell*, **34**, 151–159.
20. Evans,M.D. and Cooke,M.S. (2004) Factors contributing to the outcome of oxidative damage to nucleic acids. *Bioessays*, **26**, 533–542.
21. Cooke,M.S., Evans,M.D., Dizdaroglu,M. and Lunec,J. (2003) Oxidative DNA damage: mechanisms, mutation, and disease. *FASEB J.*, **17**, 1195–1214.
22. Amente,S., Di Palo,G., Scala,G., Castrignanò,T., Gorini,F., Coccozza,S., Moresano,A., Pucci,P., Ma,B., Stepanov,I., *et al.* (2019) Genome-wide mapping of 8-oxo-7,8-dihydro-2'-deoxyguanosine reveals accumulation of oxidatively-generated damage at DNA replication origins within transcribed long genes of mammalian cells. *Nucleic Acids Res.*, **47**, 221–236.
23. Gorini,F., Scala,G., Di Palo,G., Dellino,G.I., Coccozza,S., Pelicci,P.G., Lania,L., Majello,B. and Amente,S. (2020) The genomic landscape of 8-oxodG reveals enrichment at specific inherently fragile promoters. *Nucleic Acids Res.*, **48**, 4309–4324.
24. Scala,G., Gorini,F., Ambrosio,S., Chiariello,A.M., Nicodemi,M., Lania,L., Majello,B. and Amente,S. (2022) 8-OxodG accumulation within super-enhancers marks fragile CTCF-mediated chromatin loops. *Nucleic Acids Res.*, **42**, 3292–3306.
25. Gorini,F., Scala,G., Ambrosio,S., Majello,B. and Amente,S. (2022) OxidIP-seq for genome-wide mapping of damaged DNA containing 8-oxo-2'-deoxyguanosine. *Bio-Protocol*, **12**, e4540.
26. Dahal,S., Siddiqua,H., Katapadi,V.K., Iyer,D. and Raghavan,S.C. (2022) Characterization of G4 DNA formation in mitochondrial DNA and their potential role in mitochondrial genome instability. *FEBS J.*, **289**, 163–182.
27. Wauchope,O.R., Mitchener,M.M., Beavers,W.N., Galligan,J.J., Camarillo,J.M., Sanders,W.D., Kingsley,P.J., Shim,H.-N., Blackwell,T., Luong,T., *et al.* (2018) Oxidative stress increases M1dG, a major peroxidation-derived DNA adduct, in mitochondrial DNA. *Nucleic Acids Res.*, **46**, 3458–3467.
28. Alhagaili,A.S., Ji,Y., Sylvius,N., Blades,M.J., Karbaschi,M., Tempest,H.G., Jones,G.D.D. and Cooke,M.S. (2019) Genome-wide adductomics analysis reveals heterogeneity in the induction and loss of cyclobutane thymine dimers across both the nuclear and mitochondrial genomes. *Int. J. Mol. Sci.*, **20**, 5112.
29. Richter,C., Park,J.W. and Ames,B.N. (1988) Normal oxidative damage to mitochondrial and nuclear DNA is extensive. *Proc. Natl Acad. Sci. USA*, **85**, 6465–6467.
30. Kitsera,N., Stathis,D., Lühnsdorf,B., Müller,H., Carell,T., Epe,B. and Khobta,A. (2011) 8-Oxo-7,8-dihydroguanine in DNA does not constitute a barrier to transcription, but is converted into transcription-blocking damage by OGG1. *Nucleic Acids Res.*, **39**, 5926–5934.
31. Brueckner,F., Hennecke,U., Carell,T. and Cramer,P. (2007) CPD damage recognition by transcribing RNA polymerase II. *Science*, **315**, 859–862.
32. Cline,S.D., Lodeiro,M.F., Marnett,L.J., Cameron,C.E. and Arnold,J.J. (2010) Arrest of human mitochondrial RNA polymerase transcription by the biological aldehyde adduct of DNA, M 1 dG. *Nucleic Acids Res.*, **38**, 7546–7557.